Optimization of anti-clogging pervious pavement structure based on numerical evaluation

J. Zhang, S. Xia, N. Hu, W. Hao, R. Han, B. Meng, Z. Zhang

Amount of words：7596

Optimization of anti-clogging pervious pavement structure based on numerical evaluation

Jiong Zhang [a, b, *], Shuang Xia[a], Nian Hu[a], Wengang Hao[c, *], Ruonan Han[a], Bowen Meng[a], Zhongze Zhang[a]

[a] School of Civil Engineering, Shandong University, Jingshi Road, Jinan 250061, China
[b] Laboratoire LGCGM, INSA de Rennes, Université Européenne de Bretagne, France
[c] School of Energy and Power Engineering, Shandong University, Jingshi Road, Jinan 250061, China

ABSTRACT:

Based on numerical simulation methods, the anti-clogging performance of various pervious pavement structures were investigated. Different pavement structure models were built to analyze the effects of different pervious structures, top layer thicknesses and top aggregate gradations on the anti-clogging performance. The results shown that compared with single-layer structure, the double-layer pervious structure has better anti-clogging performance and maintenance efficiency. The most serious clogging of double-layer pervious structure can be hold within 3 mm of the superficial layer where the clogging particles can more easily be cleaned out. Smaller top layer thickness lead to a better anti-clogging performance and maintenance efficiency. And the top layer aggregate size should be selected only considering particle transport or shielding effect, based on the gradation of local clogging particles. In addition, based on the above findings, a new double-layer pervious structure with excellent anti-clogging performance has been developed, including a number of parallel vertical variable diameter tubular channels, the diameter of the upper layer is smaller than that of the lower layer.

Keywords: Pervious pavement; CFD-DEM simulation; Anti-clogging structure; Clogging depth; Clogging particles size distribution

1. Introduction

With the urbanization, impervious surfaces such as highways, streets and pavement have increased considerably, which increases the surface runoff and the risk of urban floods [1]. In order to adapt to the rapid development of urbanization, the concept of pervious pavement is proposed. It has a many number of connected pores within the aggregate skeleton. Generally, the pervious concrete is an environment friendly material with high porosity between 15% and 35%, and the initial permeability is typically about 2 - 6 mm/s even up to10 mm/s [2, 3]. High permeable capacity guarantees good drainage capacity. Therefore, pervious pavement can effectively alleviate various problems existing in the city, such as ensure driving safety [4, 5], and reduce the concentration of pollutants in runoff [6], and alleviate the current situation of groundwater shortage [7, 8]. The maximum downward seepage velocity of pervious pavement structure was less than 1% of the average runoff velocity, so the flow was considered to be uniform [9].

The effective service life of pervious pavement is directly related to its permeability, and the

clogging of pores has a serious adverse effect on the permeability of pavement [10]. Porous pervious pavement can not only reduce the road surface runoff, but also allow the runoff to carry sediments into the connected pores of pavement structure, which greatly reduces its permeability until it becomes an impermeable pavement. Through previous research, it was found that the decrease of permeability of pervious concrete caused by initial sediments could reach 50% after 2 or 3 year [11]. Kayhanian et al. [8] CT (Computed Tomography) scanned cores of pervious concrete pavements and measured the permeability to assess clogging. Walsh et al. [12] measured the effect of sediment accumulation on the hydraulic conductivity of pervious concrete in laboratory scale. Kandra et al. [13] focused on the effect of physical characteristics of filter media and flow-through rates on the clogging of stormwater filters. The clogging depth was usually concentrated in the upper layer of pervious pavement [14-16]. Other studies have observed that the clogging regions gradually occur and become stable, only the smallest clogging particles would continually transport into other places [17]. It was also found that for larger ratios, a single particle is generally not be stopped and clogging due to the arches formed when several grains attempt to go through smaller pores [17, 18]. Razzaghmanesh and Borst [19] investigated clogging dynamic of pervious pavement systems using embedded sensors and concluded that for every 6 mm of rain, clogging advanced 1 mm across the surface. The spalling of aggregate particles in porous pavement will also lead to pore clogging. Research shows that binder content and degree of compaction are the critical factors affect the raveling resistance of porous pavement structure [20].

Many numerical simulation methods were also developed to explore the hydraulic behavior and water quality performance of pervious pavement [21]. Pieralisi et al. [22] developed and validated an advanced computational fluid dynamics coupled with discrete element method (CFD-DEM) model to assess the permeability of pervious concrete. Ma et al. [23] based on virtual fatigue test, the influences by content, distribution, size and orientation of air voids on the fatigue life of asphalt mixture were evaluated by discrete element method. It was found that, higher air void content leads to lower fatigue life of asphalt mixture. Zhang et al. [24, 25] found that full-graded sands can percolate into depth of 30 mm in pervious pavement. Coarse sands can percolate in depth within 20 mm. Fine sands can percolate into the depth of 60 mm even 100 mm. Zhang et al. [25] studied the effect of the ration of the equivalent diameter of aggregate to the equivalent diameter of clogging particles on the pore clogging of pervious pavement, and found that when the ration was lower than 6.46, the clogging particles could be trapped inside the pores because they are too large to go through the smaller pores.

When the pervious pavement was clogged, the permeability can be restored to a certain extent by taking appropriate maintenance measures. Vantura et al. [26] studied the restoration of permeability of pervious pavement by vacuum hose, vacuum sweeper and regenerative air sweeper respectively. It shows that all these methods can clean clogging material in the void within the range of 3.18 mm on the surface of pervious concrete and the permeability of the pervious concrete was restored. Henderson and Tighe [27] found that in the common maintenance and cleaning measures, power spray cleaning can decrease permeability. It was also found that the combination of pressure wash and vacuum suction has the best maintenance effect, and periodic maintenance can extend the service life of pervious pavement [28].

In order to avoid the above problems, HEIJMANS road construction company in the Netherlands improves the pavement performance by using a two-layer pervious asphalt pavement consisting of fine-grained top layer and coarse-grained bottom layer [29]. The two-layer porous

asphalt concrete construction has a top layer grading 4-8 mm and bottom layer grading 11-16 mm. The top layer is similar to a sieve and acts as a filter to prevent large-size clogging particles from entering the bottom layer. At the same time, the pore diameter of the bottom layer is larger than that of the top layer, which can make the incoming fine particles discharge smoothly. Therefore, this pavement structure can maintain permeability for a longer time. In addition, the bottom structure of macropores can also avoid the decrease of permeability caused by power spray cleaning. The function of double-layer pervious structure is to improve the effectiveness and durability and reduce the clogging problem [4, 30]. The selection of the aggregate size grading of the top layer and bottom layer, especially the top layer, will directly affect the permeability of the double-layer pervious pavement. Other studies have found that the thinner the top layer, the better the cleaning effect [30]. Some studies show that the noise reduction performance of double porous asphalt pavement was improved with the decrease of aggregate size distribution of the top layer [31]. The double layer porous asphalt has a good hydrological performance, and it was able to reduce the surface runoff from a precipitation of 100 mm/h, and the sand and soil used did not significantly affect its infiltration capacity [32].

The anti-clogging effect of the double-layer pervious pavement structure has been proved by many studies. However, there is no detailed research information on the anti-clogging mechanism of the double-layer pavement, as well as the influence of specific aggregate size grading, layer thickness and other parameters. In this study, CFD-DEM coupling numerical simulation method is used to study the anti-clogging mechanism in rainfall environment. And a new tubular double-layer pervious structure is also proposed based on the simulation results. The conclusions derived from this study can contribute to the future research on construction of pervious pavement.

2. Mathematical modeling

In the CFD-DEM model, the flow in the whole flow region is calculated based on the continuity and the Naiver-Stokes equations, with a porosity term and an additional body force term used to explain the presence of particles in the fluid. The formula is as follows:

$$\frac{\partial \Phi}{\partial t} + \nabla \cdot (\Phi \vec{u}) = 0 \quad (1)$$

$$\frac{\partial (\rho \Phi \vec{u})}{\partial t} + (\nabla \cdot \vec{u})(\rho \Phi \vec{u}) = -\nabla p + \mu \nabla^2 (\Phi \vec{u}) - \sum_{i=1}^{n_v} \vec{f}_{fluid,i} + \rho \Phi \vec{g} \quad (2)$$

where ρ is the density of the fluid, Φ is the porosity, $\vec{u}$ is the fluid velocity, p is the fluid pressure, μ is the dynamic viscosity of the fluid, $\vec{g}$ is the gravitational acceleration, $\vec{f}_{fluid,i}$is the total force applied by the fluid on particle I, n_v is the number of particles per unit volume.

The porosity and body force of the fluid mesh elements are determined through DEM. The equations of motion for the particles have an additional force term to account for interaction with the fluid. The equations are given as follow:

$$m \frac{\partial \overrightarrow{u_p}}{\partial t} = \vec{f}_{mech,i} + \vec{f}_{fluid,i} + m\vec{g} \quad (3)$$

$$\frac{\partial \vec{\omega}}{\partial t} = \frac{\vec{M}}{I} \quad (4)$$

where $\overrightarrow{u_p}$ is the particle velocity, m is the particle mass, $\vec{f}_{mech,i}$ is the sum of additional forces

acting on the particle, $\vec{\omega}$ is the particle angular velocity, I is the moment of inertia, $\vec{M}$ is the torque acting on the particle.

The total force applied by the fluid on particle I, $\vec{f}_{fluid,i}$consists of two parts: drag force and a force resulting from the fluid pressure gradient. Other particle-fluid forces, such as the lift force is ignored in this study. The resulting relationship could be expressed as:

$$\vec{f}_{fluid,i} = \vec{f}_{drag,i} + \frac{4}{3}\pi r^3 \nabla p \quad (5)$$

$$\vec{f}_{drag,i} = \left(0.63 + \frac{4.8}{\sqrt{Re_{p.i}}}\right)^2 \left(\frac{1}{2}\rho\pi {r_i}^2 |\vec{u} - \vec{u}_{p,i}|(\vec{u} - \vec{u}_{p,i})\right) \Phi^{-\chi} \quad (6)$$

where the $\Phi^{-\chi}$ term is an empirical factor accounts for the local porosity, Re_p is the particle Reynolds number.

DEM and CFD two-way coupling is numerically achieved as follows: Eqs. (1) – (2) are solved with the CFD code, while Eqs. (3) – (6) are solved with DEM code. Porosity and body force are determined by DEM and divided by the volume from CFD. The fluid velocity and fluid pressure for every element are determined by the CFD and then sent to the DEM in each coupling data exchange. The coupling of CFD with DEM is realized with commercial software of Fluent and EDEM(the software for bulk material simulation) [25] in this study.

3. The setup of simulation study

3.1 The setup of DEM simulation

Both clogging particles and aggregates are generated in EDEM. During the simulation process, the fully graded clogging material designed artificially is used. The clogging particle size distribution is shown in Table 1. Fine particles account for a large proportion in the composition of the material. The clogging material can make the pervious structure completely and quickly clogged by experiment verification [28].

Table 1

Grading distribution of clogging particles.

Particle size (mm)	1.18-2.36	0.6-1.18	0.3-0.6	0.15-0.3	0.1
Particle proportion (%)	15%	20%	20%	20%	25%
Color	Pink	Blue	Green	Red	Yellow

3.1.1 Selection of aggregate size

In the double-layer pervious pavement structure, the choice of aggregate gradation has a great influence on the anti-clogging performance. There are two possibilities for the selection of aggregate size. One of which is based on the theory of Terzaghi filter layer, which needs sufficient permeability and can reduce the possibility of arching. When fine particles enter the structure, and they will drain away from the previous pavement, so they will not cause clogging. Another possibility is that the aggregate particles in the top layer can act as a shield against the clogging particles, that enhance the trapping effect of the top layer to prevent entering of clogging particles to the maximum extent. Both of considerations can minimize the occurrence of pore clogging.

In order to ensure sufficient particle transport ability, equation (7) is used to calculate the range of aggregate particle size proposed by Terzaghi. D_{15} is the particle size with cumulative

distribution of 15% in aggregate particles, and d_{15} is the particle size with cumulative distribution of 15% in clogging particles.

$$\frac{D_{15}}{d_{15}} \geq 4 \quad (7)$$

In order to maximize the shielding effect of the top layer, that most of the clogging particles can be trapped on the surface of the pavement. The pore formed by the aggregate particles is shown in Fig. 1, and the pore diameter can be calculated as follows:

$$D_p \approx (\frac{2*\sqrt{3}}{3} - 1)D \quad (8)$$

where D is the aggregate diameter, D_p is the pore diameter. If D_p is smaller than the moving particles, then all the particles can be trapped on the surface. As the aggregate particles are irregular in arrangement, the calculated result is a rough estimate.

Therefore, the design size of aggregate particles can be determined by the size of clogging particles, different clogging particle gradations will induce different aggregate gradations. For example, in this study, as Table 1 shows d_{15}=0.1 mm, the calculated D_{15}≥0.4 mm by equation (7). So, in order to ensure sufficient particle transport ability, the range of top aggregate particle size is D≥0.4 mm. While in order to keep all the clogging particles can be trapped on the surface, D_p should be smaller than 0.1 mm, then the range of top aggregate particle size should be D< 0.65 mm, if the aggregate is composed by single size particles.

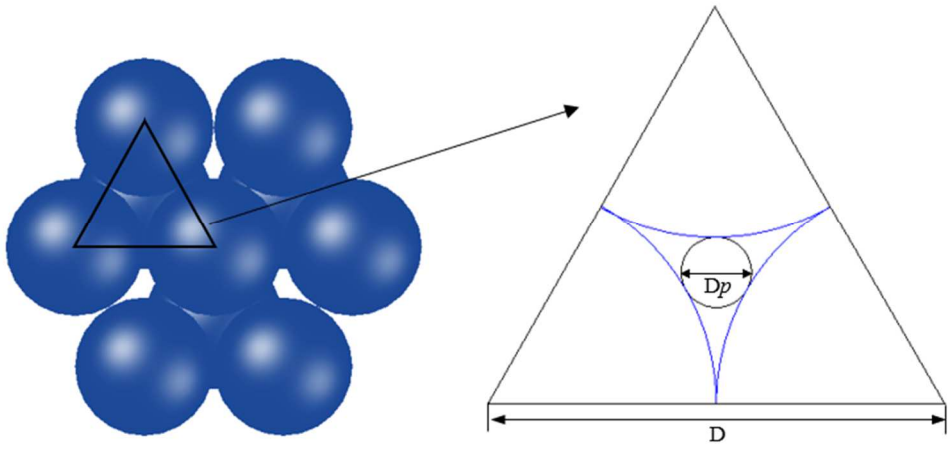

Fig.1 Pores between aggregates

Based on the above calculation, if the clogging particles is allowed to be discharged from the bottom of the pervious layer, the range of the top aggregate particle size should be D≥0.4 mm. Thus, 1 mm and 0.6 mm were taken as the top aggregate particles to meet this requirement. If all the clogging particles can be trapped by the top layer, the range of the top aggregate should be D < 0.65 mm. Therefore, 0.6 mm and 0.3 mm were chosen as the top aggregate particles to meet this requirement. The size of the bottom aggregate particles is 3 mm for all cases, which can ensure that the bottom pore is large enough and the clogging particles entering the bottom can be discharged smoothly.

3.1.2 Selection of layer thickness

It is found that the top 0-10 mm of the pavement is the most serious clogged region by experimental and numerical simulation [24, 25]. Therefore, the thickness of top layer is chosen as 10 mm, 8 mm and 5 mm for comparison and analysis. The total thickness of the pervious

pavement structure is 55 mm.

3.1.3 Model design

In order to reduce the time and costs required in the numerical simulation, the volume of pervious pavement model is fixed and its length, width, and thickness is 20 × 20 × 55 mm. Particle accumulation theory indicates that when a single particle size is randomly filled, the average porosity is 0.359-0.375. Due to the influence of wall effect, the porosity is uniformly 0.39 in this study. Total volume of aggregates and cement paste used in pervious pavement model is calculated by the equation $V_{ac} = V \times (1 - P)$, where V_{ac} is the total volume of aggregates and cement paste, V is the volume of pervious pavement, P is the porosity of pervious pavement. In order to simplify this model, the cement paste volume is directly incorporated into the aggregate volume, using only single-phase aggregate particles in pervious pavement model.

According to the above discussion of aggregate size and top layer thickness, 6 models were established according to the structure type, top layer thickness and aggregate gradation (Table 2). The control group was single-layer structure and the other five models were double-layer structure.

Table 2

Pervious pavement structure model

Model		Control group	U1-10	U1-8	U1-5	U0.6-5	U0.3-5
Aggregate size (mm)	Top layer	3	1	1	1	0.6	0.3
	Bottom layer		3	3	3	3	3
Thickness (mm)	Top layer	55	10	8	5	5	5
	Bottom layer		45	47	50	50	50

As shown in Table 3, the basic parameter settings of each type of particle. The Poisson's ratio of aggregate particles is 0.3, the shear modulus is 1.85e + 06 Pa, and the density is 2450 kg/m³; the Poisson's ratio of clogging particles is 0.3, the shear modulus is 1.85e + 06 Pa, and the density is 2650 kg/m³. The restitution coefficient between particles is 0.001, the static friction coefficient is 0.5, and the rolling friction coefficient is 0.2. In particular, the shear modulus of the simulated material is usually much smaller than the actual value to increase the time step used for simulations. This leads to larger overlaps between particles but does not change the overall behavior of clogging in pervious pavement model.

Table 3

Basic parameter setting of particles

Particles	Poisson's ratio	Shear modulus	Density
Aggregate particles	0.3	1.85E+06 Pa	2450 kg/m³
Clogging particles	0.3	1.85E+06 Pa	2650 kg/m³
Contact parameters	Coefficient of restitution	Coefficient of static friction	Coefficient of rolling friction

Particle-Particle	0.001	0.5	0.2

When establishing the model in EDEM software, aggregate particles are randomly generated by the Particle-factory and compacted with plates to closely fill them to achieve the required porosity. The BPM (bonded particle model) model is applied to remedy the drawback that lacks cement paste. It is added to aggregate particles to bond them as a whole pervious pavement model under the cohesive force. When bonding particles with BPM model, the normal stress and shear stress are set at 2e+07 N/m, and the critical normal stress and the critical shear stress are set at 5e+30 Pa. Both the critical normal stress and the critical shear stress are much larger than the actual critical value in order to prevent the structure from being destroyed, as the clogging behavior is the primary goal of this study rather than the mechanical behavior. When bonding aggregate particles, the time step should be about 10% of Rayleigh time step.

3.2 The setup of CFD-DEM coupling model

After the DEM model is established, the coupling setup with CFD is performed. During the coupling process, the grid size in Fluent should be greater than or equal to the largest particle size in EDEM. It has been pointed out that when the size of the mesh is slightly smaller than the fixed particle size and larger than the movable particle size, it has little influence on the analysis of the movement and position of the clogging particles [33]. Therefore, the mesh size used in this simulation is 3 mm, and the outlet position has been encrypted to some extent. This meets the size requirements of the CFD-DEM coupling to the grid. Fig.2 shows the grid used in the coupling process, gray represents the wall, blue represents the inlet, and red represents the outlet.

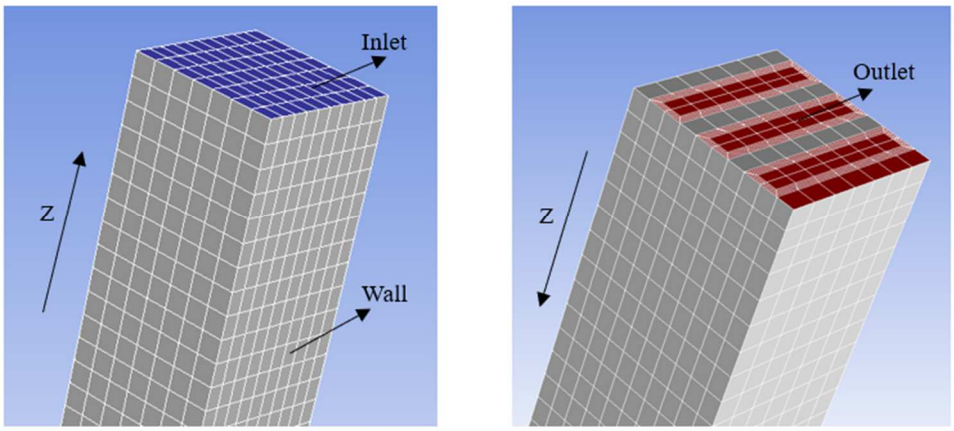

Fig.2 CFD grid model

As shown in Fig.3, the CFD-DEM coupling model simulates the rapid clogging process of pervious pavement under rainfall conditions. The standard *k-ε* turbulence model and PISO (Pressure Implicit with Splitting of Operator) method are used to simulate rainfall in Fluent. In the setting of boundary conditions, the inlet is set as the velocity inlet, the flow rate is set as 0.03 m/s and the outlet is set as the pressure outlet. Water flows from the inlet to the outlet in the -Z direction.

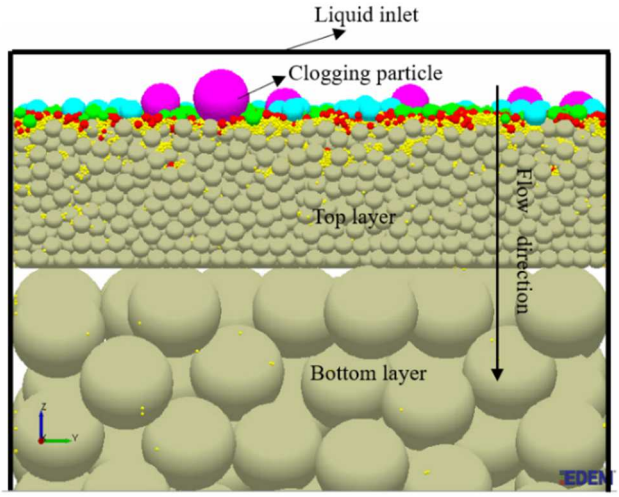

Fig.3 CFD-DEM coupling model

During the coupling calculation, the whole process is carried out for 7s. 0-0.5s is the process of adding clogging particles. Some fine-sized clogging particles directly enter the pore structure under the action of gravity. After 0.5s, rapid clogged under the condition of rainfall begins. The calculation time step of CFD is 5×10^{-4}s and that of DEM is 2×10^{-6}s (31% Rayleigh time step). During the coupling process, the structure of the pervious pavement remains stationary, and the clogging particles move under the action of gravity and water flow. Some of the clogging particles are trapped on the surface of the structure. Some of the clogging particles eventually pass through the structure model of the pervious pavement and are carried away by water flow. Otherwise, some of the clogging particles are trapped in the pores, which reduces the permeability of the pervious pavement.

4. Results and discussion

Surface sediments can be easily cleaned up when conducting pervious structure clogging experiments indoors. However, it is difficult to achieve the clearing operation in the process of EDEM simulation. Therefore, in the process of analyzing the clogging particle volume data, the clogging particle volume remaining in the depth of structure surface (the depth of half aggregate particle size) is not considered, and the clogging particle in this thickness can be easily removed. Thus, the volume of clogging particles in the effective thickness of each model (total thickness minus half aggregate particle size at the top of the model) is selected for analysis.

4.1 Development of clogging in pervious structure

Fig. 4 shows the movement of clogging particles of different particle sizes over time within the depth of 0-15 mm on the pervious structure surface. Fig. 4 (a) represents a single-layer pervious structure, and Fig. 4 (b) represents a double-layered pervious structure.

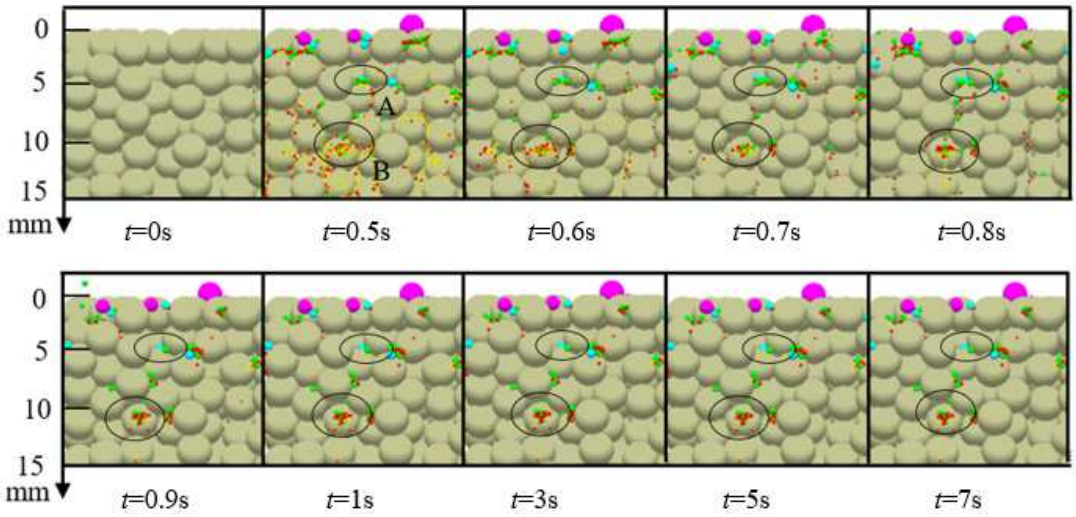

(a) Single-layer structure: control group

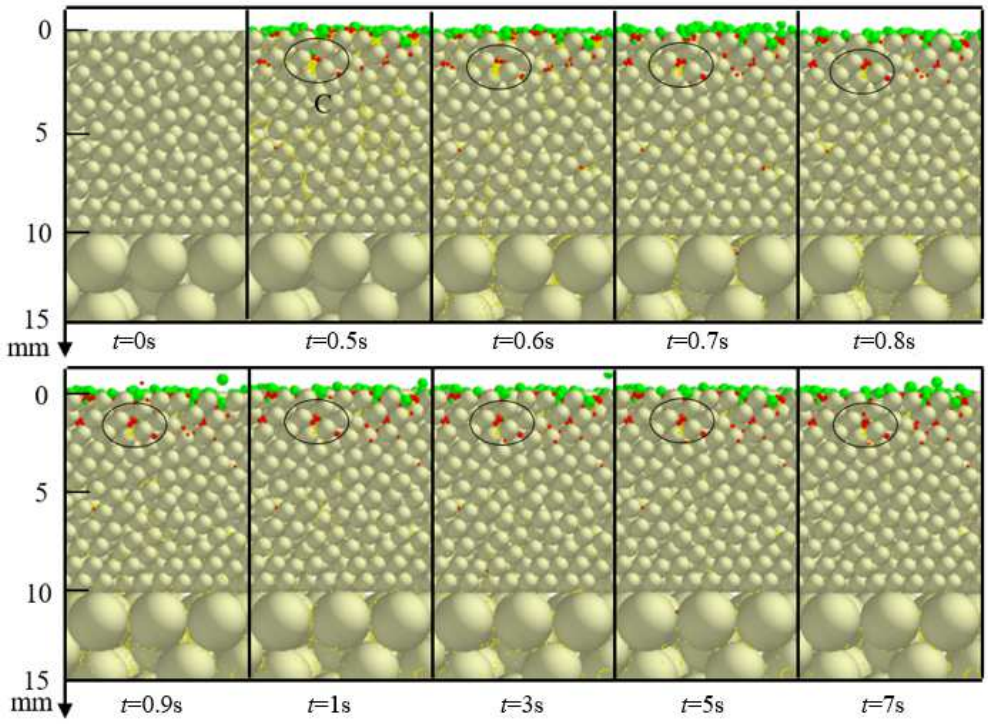

(b) Double-layer structure: U1-10

Fig. 4 Movement of clogging particles in pervious structure

Fig. 4 (a), shows that in addition to the largest particle (i.e. pink, *d*s=1.18-2.36 mm), the rest particles enter into the structure. In region A (the depth of 5 mm in pervious pavement), the blue clogging particles (*d*s=0.6-1.18 mm) are involved. They are mainly settled on shallow surface within depth of 5 mm, and a few blue particles could percolate down to the depth of 10 mm. This bule particles deposit into the pores and becomes new skeleton particles. This causes some pore channels of pervious pavement suddenly get narrow. Over time, it is easy to accumulate other small size of clogging particles around it and clog the pore.

There is no large diameter clogging particles in region B (the depth of 10 mm in pervious pavement). Green (*d*s=0.3-0.6 mm), red (*d*s=0.15-0.3 mm) and yellow (*d*s=0.1 mm) clogging particles transport deeply under the effect of seepage flow. Yellow particles basically do not

deposit in the pore, some red and green particles can gather to clog the pore.

In Fig. 4 (b), as shown in regional C (the depth of 2 mm in pervious pavement). It can be found that only red and yellow two small sizes of sediments can enter the pores in the top layer of the double-layer pervious structure, while the others are left outside the structure. The red particles are mainly settle on shallow surface of 3 mm depth. This red particles remaining in the pore become new skeleton particles. Over time, the small yellow particles will gather around and slowly block the pore.

Thus, in the single-layer pervious structure, it is found that there are many kinds of clogging particles which can enter the pore, and the percolate depth is deeper. In the double-layer pervious structure, due to the shielding effect of the top structure, the types of clogging particles that can enter the pore and the depth of entry are reduced, and the possibility of forming complex particle groups between clogging particles is greatly reduced.

Furthermore, in order to study the development of clogging at different depth region of each pervious structure, the models are divided into five layers by the depth, which are layer I (0-3 mm), II (3-5 mm), III (5-10 mm), IV (10-30 mm), and V (30-55 mm) respectively. The variation processes of the volume of clogged particles in each layer compared to the total volume of the layer, i.e. clogged particle volume fraction, are shown in Fig. 5.

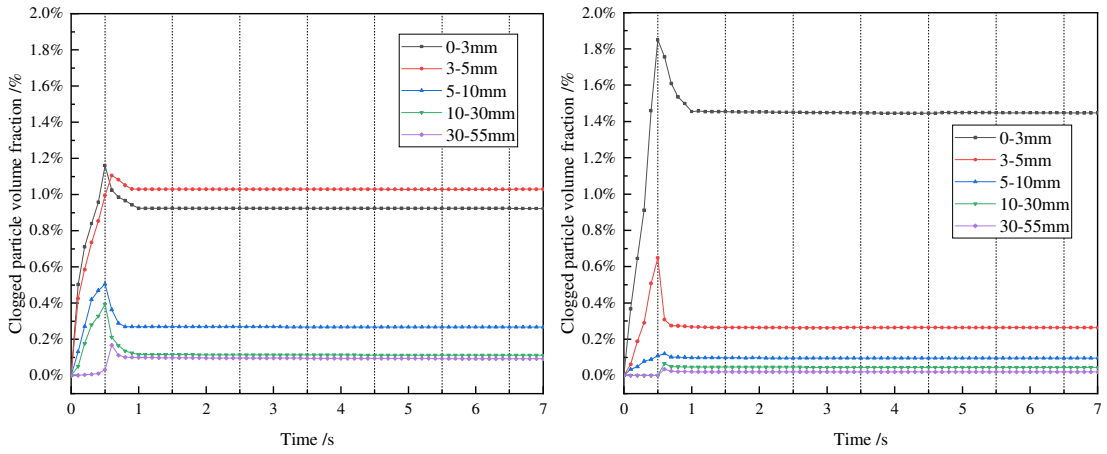

(a) Control group (b) U1-10

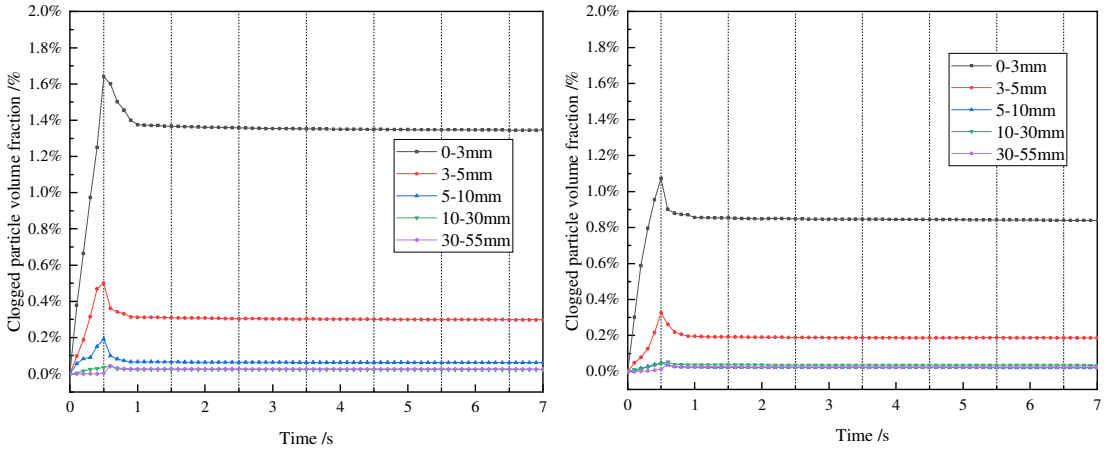

(c) U1-8 (d) U1-5

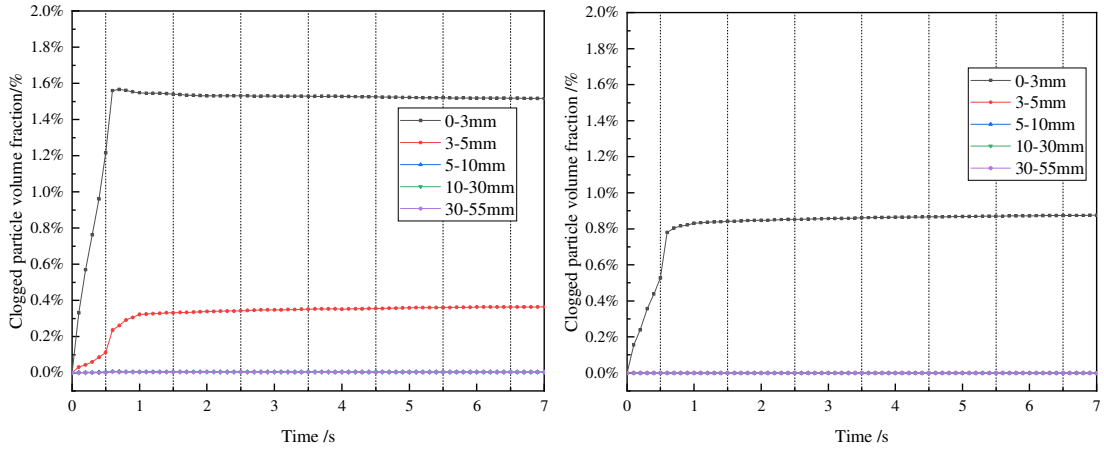

(e) U0.6-5 (f) U0.3-5

Fig. 5 Clogging development process in different layers

4.1.1 The influence of single- and double-layer structure

As shown in Fig. 5 (a) and (b), we can find that the trend of the volume fractions of clogged particles in most layer is upward within 0-0.5s and downward after 0.5s, then tends to be stable. The main reason is that before the rainfall, some small size clogged particles enter the pore structure under the action of gravity, and the volume fractions increases. Afterwards, due to the effect of seepage flow, these small particles continue to move downwards and the volume fractions decreases, finally gradually becoming stable.

In Fig. 5 (a) and (b), comparing the layers I and II of the control group, it can be found that after 0.55s, the volume fraction of clogged particles in layer II is larger than layer I. This is due to the early rainfall, layer I of clogged particles are transported to the layer II quickly under the effect of seepage flow. In the layer II the clogged particles quickly gathered, the seepage flow effect gradually decreased, clogging particles transported speed becomes slower. Finally, the volume fractions of clogged particles in layer II is larger than layer I. The volume fractions of clogged particle in layer I of U1-10 structure is much larger than that in other layers of U1-10 and also larger than that in the layers I and II of control group. In addition, the volume fractions of clogged particles in the layers II and III of U1-10 is one-fourth of control group. This indicates that the most of clogged particles can be hold within 3 mm of the superficial layer of the double-layer structure.

Through comparative analysis, it is shown that the shielding effect of the double-layer structure is obvious, and the clogged particles can be hold within 3 mm of the superficial layer, which cannot cause serious clogging problems in deep layers, and reduce the difficulty of maintenance.

4.1.2 The influence of top thickness of double-layer pervious structure

In Fig. 5 (b), (c) and (d), the clogging development process of the double-layer pervious structure with a top layer thickness of 10, 8 and 5 mm is shown respectively. It can be found that the layers with the largest volume fractions of clogged particles in the three structures is the layer I, and followed by layer II. And the volume fractions are very small in the other three layers. However, the volume fractions of clogged particles in the layers I and II of U1-5 are only half of those in U1-10 and U1-8, and particles clogged in the other layers also reduce. Therefore, with the decrease of the top layer thickness, the volume fractions of the clogged particles in each layer

decreases, and the anti-clogging performance of the structure improves.

4.1.3 The influence of aggregate gradation on top layer

In Fig. 5 (d), (e) and (f), the clogged development processes of the double-layer pervious structures with 1, 0.6, and 0.3 mm particle size of the top aggregate are respectively represented. It can be found that in the U0.6-5 and U0.3-5 structures, there are no obvious decrease trend of the volume fractions of clogged particles, but only rises and finally tends to stabilize. This is because with the decrease of the top aggregate size, the pore diameter of the structure decreases, and the shielding effect increases. The clogged particles can only move slowly and are difficult to enter deeper layers, even under the action of seepage flow.

By comparing the layers where clogged particles exist in each structure, it is found that clogged particles exist in all layers in the U1-5 structure, while only two layers in the U0.6-5, which are layers I and II, and only one layer in the U0.3-5, which is layer I. This means that as the top aggregate size decreases, the accessible depth of the clogged particles decrease.

In the layers I and II of U0.6-5, the volume fractions of clogged particles increase compared with that in the same layers of U1-5. The reason is that with the decrease of top aggregate size, shielding effect increases very slightly, which results in the gradual accumulation clogged particles. While for U0.3-5, when the top aggregate size is further decreases, the shielding effect is greatly enhanced and plays a major role. Therefore, the volume fractions of clogged particles in the layer I decreases. More detailed analysis can be found in section 4.2.3.

4.2 Analysis on final clogged state of pervious pavement structure

After clogging becomes stable, the total volume of clogged particles trapped inside the pore structure of each model is shown in Fig. 6 to compare the anti-clogging performance of each model. Fig.7 demonstrates the distribution of clogged particles in different layers of each models.

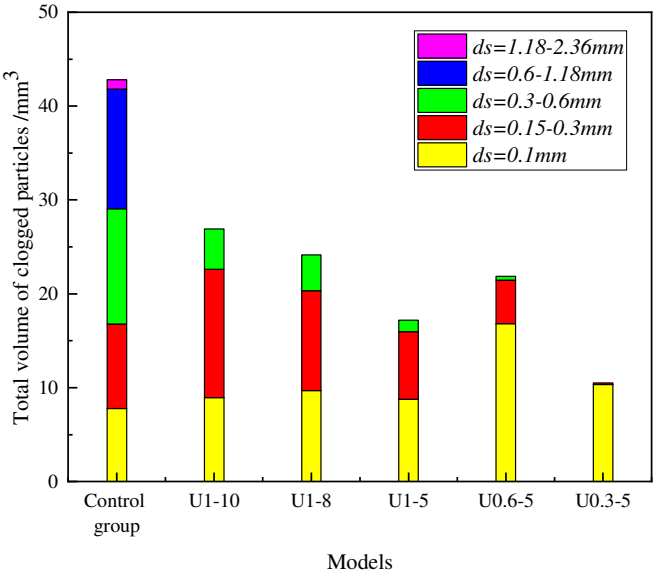

Fig.6 Volume of clogged particles with different sizes in each model

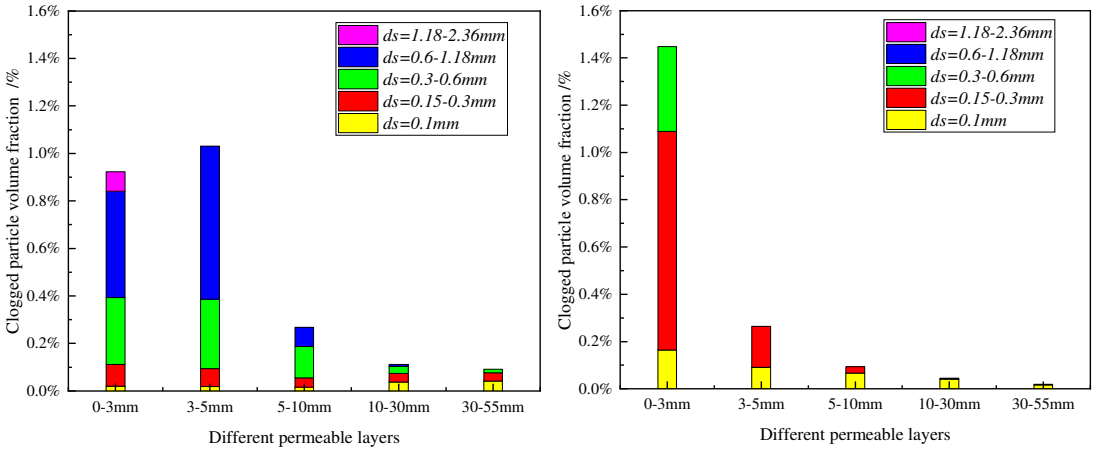

(a) Control group (b) U1-10

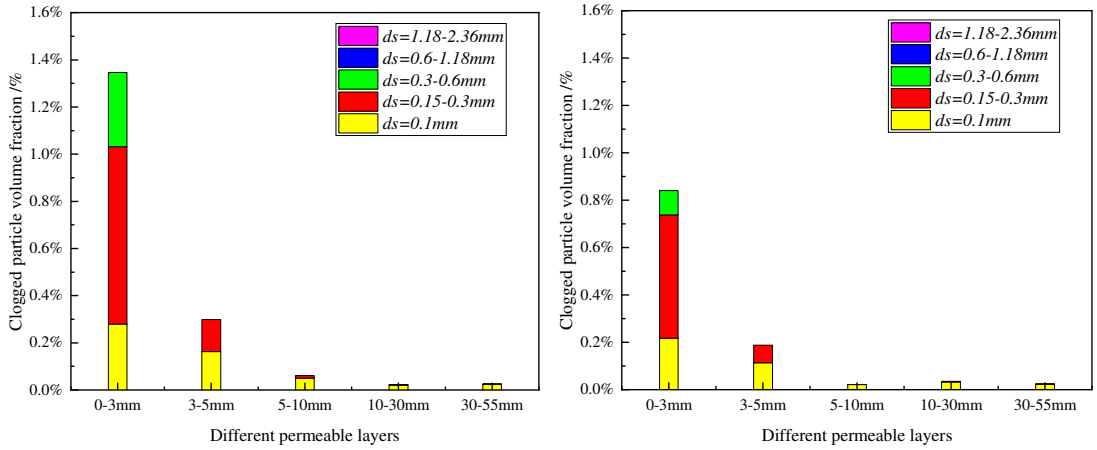

(c) U1-8 (d) U1-5

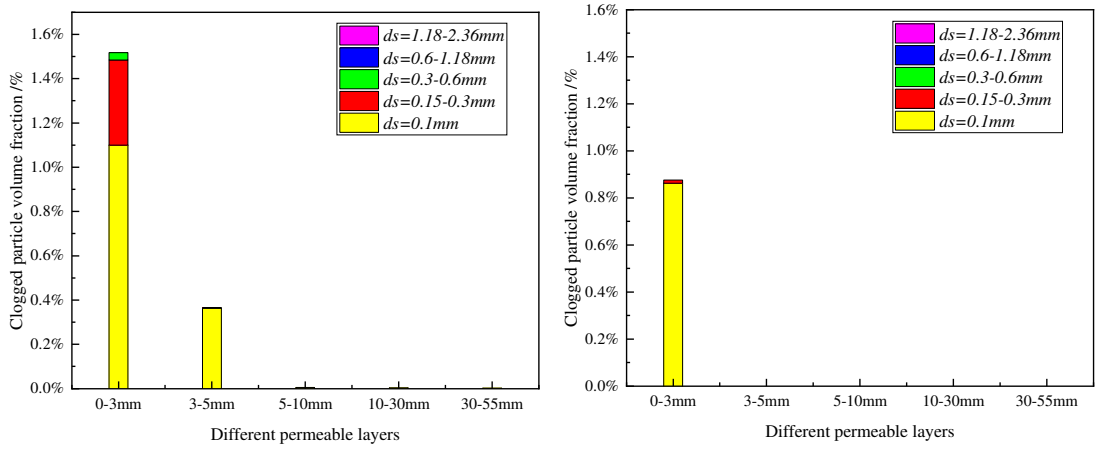

(e) U0.6-5 (f) U0.3-5

Fig. 7 Distribution of clogging particles in different layers

4.2.1 The influence of single- and double-layer structure

As shown in Fig. 6, the total volume of clogged particles in the control group is the largest compared with all other structures, and all kinds of particles exist. Besides the largest particles (i.e. pink, *d*s=1.18-2.36 mm), the volume of other clogged particles whose size range from 0.1 to 1.18 mm are roughly the same. It indicates that in the control group, the kind of clogged particles is

complex, and the clogged volume is large. Meanwhile, it can be found that the volume of clogged particles in U1-10 is reduced by 37.08%, U1-8 by 43.59%, U1-5 by 59.81%, U0.6-5 by 48.92% and U0.3-5 by 75.45% compared with the control group. Therefore, single-layer structure has the worst anti-clogging performance.

As shown in Fig. 7 (a). It is found that in the layers I and II of the control group, the largest clogged volume fraction is caused by blue (ds=0.6-1.18 mm) particles, followed by green (ds=0.3-0.6 mm); The other three layers have 3-4 kinds of clogging particles but the total clogged volume fraction is small. The pink (ds=1.18-2.36 mm) particles could be transported down to the depth of 3 mm (Layer I), and blue (ds=0.6-1.18 mm) particles could be transported down to the depth of 30 mm (Layers I - IV). The particles size range from 0.1 mm to 0.6 mm could be transported to the depth of 55 mm (Layers I - V). However, as shown in Fig. 7 (b), the large particles such as pink (ds=1.18-2.36 mm) and blue (ds=0.6-1.18 mm) are not able to enter the pore of double-layer pervious structure. In the layer I of U1-10, the largest clogged volume fraction is caused by red (ds=0.15-0.3 mm) particles, followed by green (ds=0.3-0.6 mm). The other four layers only have 1-2 kinds of clogging particles and the total volume fraction is small. The green (ds=0.3-0.6 mm) particles could enter the depth of 3 mm (Layers I - IV), and red (ds=0.15-0.3 mm) particles could enter the depth of 10 mm (Layers I - III). Only the yellow (ds=0.1 mm) particles could enter the depth of 55 mm (Layers I - V). The clogged volume fraction in the layer I of the U1-10 is larger than that of the control group, but the other four layers are smaller than that of the control group.

Therefore, compared with the single-layer pervious structure, the total clogged volume fraction of the double-layer pervious structure is smaller, and the size of the clogged particles in each layer becomes smaller. Therefore double-layer pervious structure has better anti-clogging performance.

4.2.2 The influence of top thickness of double-layer pervious structure

As shown in Fig. 6 and Fig. 7 (b), (c) and (d), it is found that the size distribution of clogged particles are roughly the same in each layer of the U1-10, U1-8, U1-5 structures, and the size distributions get narrower with the increase of the depth. The green (ds=0.3-0.6 mm) particles are not able to move deeper, they stop in the layer I. The red (ds=0.15-0.3 mm) particles could be transported to the depth of 10 mm (Layers I - III) in the U1-10 and U1-8, but they are stopped at depth of 5 mm (Layers I - II) in the U1-5. It indicates that as the thickness of the top layer decreases, the volume fraction of green and red clogged particles decreases and the total volume fraction decreases in the each layer. Therefore, the anti-clogging performance of the double-layer permeable structure improves with the decrease of the top layer thickness.

4.2.3 The influence of aggregate gradation on top layer

As shown in Fig. 7 (d), (e) and (f), it is found that the green (ds=0.3-0.6 mm) particles could enter the depth of 3 mm (Layer I) in the U1-5 and U0.6-5. The red (ds=0.15-0.3 mm) particles could enter the depth of 5 mm (Layers I - II) in the U1-5, but it could enter the depth of 3 mm (Layer I) in the U0.6-5, the green (ds=0.3-0.6 mm) and red (ds=0.15-0.3 mm) particles are not able to enter the pores of U0.3-5. The yellow (ds=0.1 mm) particles could enter the depth of 55 mm (Layers I - V) in the U1-5, but they are stopped at the depth of 5 mm (Layers I - II) in the U0.6-5, and they are stopped at the depth of 3 mm (Layer I) in the U0.3-5. It shows that with the decrease of the top aggregate size, the shielding effect of the double-layer structure increases.

Meanwhile, the size distribution of clogged particles narrows in the same layer.

In Fig. 6 and Fig. 7, it can be found that there are three kinds of clogging particles in U0.6-5, which are green (*d*s=0.3-0.6 mm), red (*d*s=0.15-0.3 mm), and yellow (*d*s=0.1 mm), and there is only one kind of particles in U0.3-5, which is yellow (*d*s=0.1 mm). The total volume of clogged particles in U0.6-5 is more than that of U1-5 and U0.3-5, because of the accumulation of yellow (*d*s=0.1 mm) particles in the pores of U0.6-5. The aggregate size of U0.6-5 structure is greater than 0.4 mm and less than 0.65 mm, as analyzed in section 3.1.1, which achieves both goals at the same time, e.g. shielding effect and ensuring particle transport ability. But the results show that while the shielding effect on green (*d*s=0.3-0.6 mm) and red (*d*s=0.15-0.3 mm) particles is enhanced, the yellow (*d*s=0.1 mm) particles are not shielded, and meanwhile their transport in pore is greatly restricted, which finally leads to large accumulation of yellow particles in the pores of the U0.6-5. Compared with U1-5 and U0.3-5 structures, U0.6-5 has either particle transport or shielding capabilities for yellow (*d*s=0.1 mm) particles.

Therefore, in order to enhance the anti-clogging performance of the double-layer permeable structure, the top aggregate size should be selected only considering one of the factors, either particle transport or shielding effect, based on the gradation of local clogging particles.

4.3 The maintenance efficiency of different pervious structures

In order to study the maintenance efficiency of different pervious pavement structures, the clogging-maintenance cycle is carried out with the numerical simulation. The maintenance measure adopted is vacuum suction. The vacuum suction pressure is 0.05 MPa and the suction time is 1s. The comparation of multi cycle maintenance efficiency of different models are shown in Fig. 8.

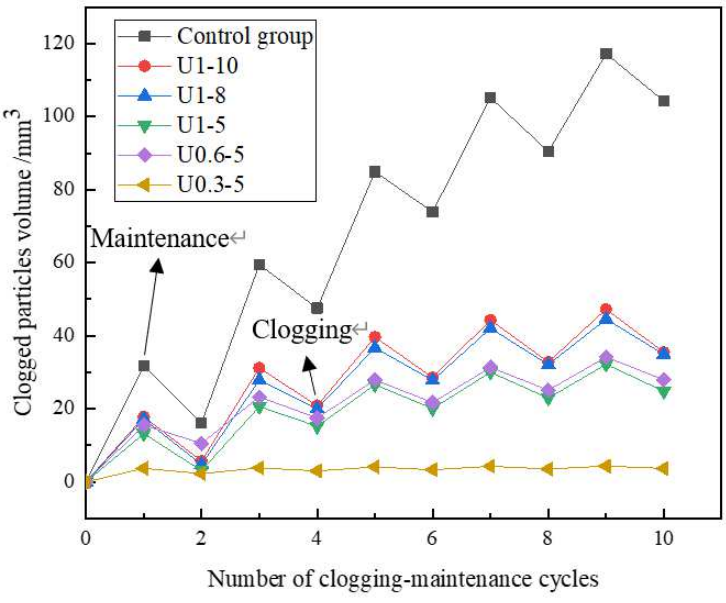

Fig. 8 Clogging of different pervious pavement structures after clogging-maintenance cycles

As shown in Fig. 8, it can be found that the clogged of each structure has been restored to a certain extent after each maintenance, but the recovery result is different. The clogged particles volume finally presents an upward trend in the structures. With the increase of the number of cycles, the upward trend of the control group is the most obvious, and the volume of clogged particles increases sharply, the maintenance effect is not good. Therefore, under the same

conditions, the single-layer pervious structure will first reach a completely clogged state, and the effective service life will be short. In the double-layer pervious structure, with the increase of the number of cycles, the volume of clogged particles increases very gently, and the maintenance effect is very good. Compared with U1-10 and U1-8, the U1-5, as the thickness of the top layer decreases, the maintenance efficiency and effective life increase. It is consistent with the conclusion of Hamzah et al. [30]. U0.3-5 structure has no obvious upward trend in the volume of clogged particles after several clogging cycles due to its strong shielding effect, and has good anti-clogging ability.

4.4 A new double-layer pervious structure

Pore structure of common pervious pavement is characterized by high tortuosity, variable diameter section and pore throat, which are the main reasons for clogging of pervious pavement. Therefore, a new tubular double-layer pervious structure with no curved channels has been developed, based on the above investigation on the anti-clogging ability of the double-layer pervious pavement structure. As shown in Fig. 9, A and B represent interconnected tubular pore with different diameters, which concentrate the pores together, giving them low tortuosity, uniform cross-section and no pore throat. According to the above aggregate size analysis, in order to ensure its permeability and shielding effect, the pore diameter of the top layer is 1 mm, the bottom layer is 3 mm, the thickness of the top layer is 10 mm and the bottom layer is 45 mm. In addition, the spacing of the top tubular pore is 4 mm to ensure that its porosity is similar to the above structures (P=0.39).

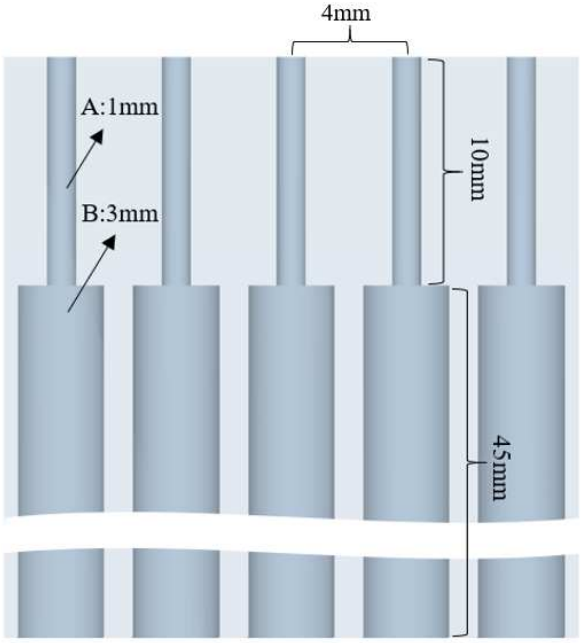

Fig.9 New tubular double-layer pervious structure

The clogging experiment to the new developed structure has also been carried out. Fig.10 (a) shows the movement of the clogging particles in the simulation process, and Fig.10 (b) and (c) are the cross-sectional and top views of the structure after clogging is stable. It is found that the new tubular double-layer pervious structure will not trap the clogging particles in the pore due to its own structural characteristics (the clogging particle model used in the simulation is regular spherical), which ensures the anti-clogging property of the structure to the maximum extent and

extends the effective service life greatly. In actual construction, the new developed pervious structure can be prefabricated in factories (Fig. 11 is a resin model), and paved on site. More investigation of the performance of this new developed pervious structure, such as the relationship of the porosity and strength will be carried out in the further study.

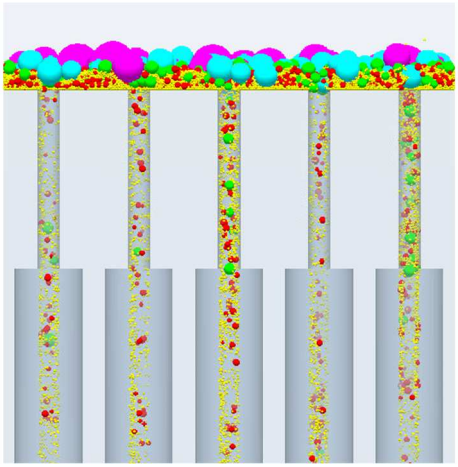

(a) Clogging particles movement

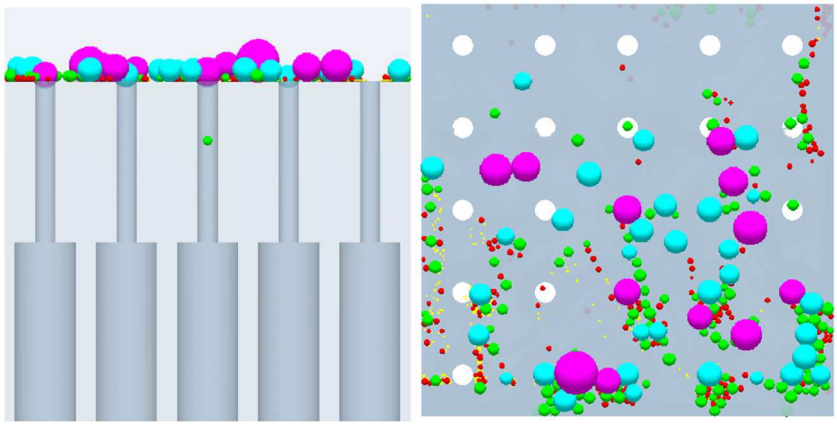

(b) Cross-section View (c) Top view

Fig.10 Clogging process of new developed pervious structure

Fig.11 A resin model of the new developed pervious structure

5. Conclusion

Through CFD-DEM coupling method, 7 different models were established to analyze the effects of different structure types, top layer thicknesses and top aggregate sizes on the anti-clogging performance of the pervious pavement structure. The conclusions are as follows:

1. Compared with the single-layer pervious pavement structure, the total clogged volume fraction of the double-layer pervious structure is smaller, and the size distribution of clogged particles narrows in each layer. Therefore, the double-layer pervious pavement has better anti-clogging performance. Meanwhile the maintenance efficiency and effective service life of double-layer pervious pavement are greater than that of single-layer.
2. For the double-layer pervious pavement structure, due to the shielding effect of the top layer, the most serious clogged of the double-layer pervious structure were 0-3 mm below the pavement surface, followed by 3-5 mm. Therefore, the double-layer pervious pavement structure reduces the depth of clogging.
3. For the double-layer pervious pavement structure, with the decrease of top layer thickness, the volume fractions of the clogged particles in each layer decreases, the anti-clogging performance improves. Meanwhile with the decrease of top layer thickness, the maintenance efficiency is improved and effective life is prolonged. The results show that the top layer thickness of 5 mm has the best the anti-clogging performance in this study.
4. For the double-layer pervious pavement structure, as the top aggregate size decreases, the shielding effect increases, and the accessible depth of the clogged particles decrease. The results show that the top layer aggregate size of 0.3 mm has the best the anti-clogging performance in this study.
5. In addition, the design size of top aggregate particles can be determined by the size of clogging particles, different clogging particle gradations will induce different aggregate gradations. The results showed that the top aggregate size should be selected only considering particle transport or shielding effect, based on the gradation of local clogging particles.
6. A new tubular double-layer pervious structure has been invented and studied, which has excellent anti-clogging performance due to its unique pore structure. The new developed pervious structure can be prefabricated and paved on site in real application cases.

6. Acknowledgements

The authors would like to thank the National Key Research and Development Project(2018YFB1600100), Natural Science Foundations of Shandong Province, China (Nos. 2017GSF22101, and ZR2018MEE046) and the Fundamental Research Funds for the Central Universities (No.2018JC040).

7. References:

[1]. Zhu, H., et al., Simulation Study on Effect of Permeable Pavement on Reducing Flood Risk of Urban Runoff. International Journal of Transportation Science & Technology, 2019.

[2]. Montes, F. and L. Haselbach, Measuring hydraulic conductivity in pervious concrete. Environmental Engineering Science, 2006. 23(6): p. 960-969.

[3]. Paul D. Tennis, M.L.L.A., Pervious Concrete Pavements. 2004.

[4]. Liu, M., X. Huang and G. Xue, Effects of double layer porous asphalt pavement of urban streets on noise reduction. International journal of sustainable built environment, 2016. 5(1): p. 183-196.

[5].Mullaney, J. and T. Lucke, Practical Review of Pervious Pavement Designs. Clean-soil Air Water,

2014. 42(2): p. 111-124.
[6]. Pagotto, C., M. Legret and P.L. Cloirec, Comparison of the hydraulic behaviour and the quality of highway runoff water according to the type of pavement. Water Research, 2000. 34(18): p. 4446-4454.
[7]. Sansalone, J.J., et al., Filtration and clogging of permeable pavement loaded by urban drainage. Water Research, 2012. 46(20): p. 6763-6774.
[8]. Kayhanian, M., et al., Permeability measurement and scan imaging to assess clogging of pervious concrete pavements in parking lots. Journal of Environmental Management, 2012. 95(1): p. 114-123.
[9]. Zhang, J., et al., Sediment transport and pore clogging of a porous pavement under surface runoff. Road Materials and Pavement Design, 2017. 18(sup3): p. 240-248.
[10]. Lu, G., et al., Development of a sustainable pervious pavement material using recycled ceramic aggregate and bio-based polyurethane binder. Journal of Cleaner Production, 2019. 220: p. 1052-1060.
[11]. Balades, J., M. Legret and H. Madiec, Permeable pavements: pollution management tools. Water Science and Technology, 1995. 32(1): p. 49-56.
[12]. Walsh, S.P., A.A. Rowe and Q. Guo, Laboratory Scale Study to Quantify the Effect of Sediment Accumulation on the Hydraulic Conductivity of Pervious Concrete. Journal of Irrigation and Drainage Engineering-asce, 2014. 140(6): p. 04014014.
[13]. Kandra, H.S., et al., Assessment of clogging phenomena in granular filter media used for stormwater treatment. Journal of Hydrology, 2014. 512: p. 518-527.
[14]. Bean, E.Z., W.F. Hunt and D. Bidelspach, Field Survey of Permeable Pavement Surface Infiltration Rates. Journal of Irrigation and Drainage Engineering-asce, 2007. 133(3): p. 249-255.
[15]. Haselbach, L., S. Valavala and F. Montes, Permeability predictions for sand-clogged Portland cement pervious concrete pavement systems. Journal of Environmental Management, 2006. 81(1): p. 42-49.
[16]. Yong, C.F., D.T. Mccarthy and A. Deletic, Predicting physical clogging of porous and permeable pavements. Journal of Hydrology, 2013. 481: p. 48-55.
[17]. Remond, S., DEM simulation of small particles clogging in the packing of large beads. Physica A-statistical Mechanics and Its Applications, 2010. 389(21): p. 4485-4496.
[18]. Li, H. and A.P. Davis, Urban Particle Capture in Bioretention Media. II: Theory and Model Development. Journal of Environmental Engineering, 2008. 134(6): p. 419-432.
[19]. Razzaghmanesh, M. and M. Borst, Investigation clogging dynamic of permeable pavement systems using embedded sensors. Journal of Hydrology, 2018. 557: p. 887-896.
[20]. Wang, D., et al., Effects of Material Composition on Mechanical and Acoustic Performance of PoroElastic Road Surface (PERS). construction and building materials, 2017. 135: p. 352-360.
[21]. Pieralisi, R., S.H.P. Cavalaro and A. Aguado, Discrete element modelling of the fresh state behavior of pervious concrete. Cement and Concrete Research, 2016. 90: p. 6-18.
[22]. Pieralisi, R., S.H.P. Cavalaro and A. Aguado, Advanced numerical assessment of the permeability of pervious concrete. Cement and Concrete Research, 2017. 102: p. 149-160.
[23]. Ma, T., et al., Influences by air voids on fatigue life of asphalt mixture based on discrete element method. construction and building materials, 2016. 126: p. 785-799.
[24]. Zhang, J., et al., Experimental simulation study on pore clogging mechanism of porous pavement. Construction and Building Materials, 2018. 187: p. 803-818.
[25]. Zhang, J., et al., Numerical study on pore clogging mechanism in pervious pavements. Journal of Hydrology, 2018. 565: p. 589-598.
[26]. Vancura, M.E., K. MacDonald and L. Khazanovich, Location and Depth of Pervious Concrete

569 Clogging Material before and after Void Maintenance with Common Municipal Utility Vehicles.
570 journal of transportation engineering asce, 2012. 138(3): p. 332-338.
571 [27]. HendersonVimy and L. TigheSusan, Evaluation of pervious concrete pavement permeability
572 renewal maintenance methods at field sites in Canada. canadian journal of civil engineering, 2011.
573 [28]. Hu, N., et al., A field performance evaluation of the periodic maintenance for pervious concrete
574 pavement. journal of cleaner production, 2020. 263.
575 [29]. Bochove, V. and G. G, TWINLAY, A NEW CONCEPT OF DRAINAGE ASPHALT
576 CONCRETE. 1996.
577 [30]. Hamzah, M.O., et al., Laboratory simulation of the clogging behaviour of single-layer and
578 two-layer porous asphalt. Road Materials and Pavement Design, 2013. 14(1): p. 107-125.
579 [31]. Kuijpers, A. and G. Blokland, Modeling and optimization of two-layer porous asphalt roads.
580 2000.
581 [32]. Afonso, M.L., C. Fael and M. Dinisalmeida, Influence of clogging on the hydrologic performance
582 of a double layer porous asphalt. International Journal of Pavement Engineering, 2018: p. 1-10.
583 [33]. Ma, G., et al., Reply to the Comment on “Numerical study on pore clogging mechanism in
584 pervious pavements”. Journal of Hydrology, 2019. 578: p. 124050.